

Effects of Precipitation pH Values on the Electrochemical Properties of β -Nickel Hydroxide Materials

C.R. Ravi Kumar^{1,4}, P. Kotteeswaran², V. Bheema Raju³, A. Murugan⁴, M.S. Santosh⁵, H. P. Nagaswarupa¹, S.C. Prashantha¹, M.R. Anil Kumar¹

¹Research Center, Department of Science, East West Institute of Technology, Bangalore-560091, India.

²Department of Chemistry, Renganayagi Varatharaj College of Engineering, Salvarpatti, Tamilnadu 626128, India

³Department of Chemistry, Dr. Ambedkar Institute of Technology, Bangalore 560 056, India

⁴Department of Chemistry, Kalasalingam University, Anandnagar, Srivilliputtur-626126, Tamilnadu, India

⁵Centre for Emerging Technologies, Jain University, Jain Global Campus, 45th km, NH-209, Jakkasandra Post, Kanakapura Taluk, Ramanagaram 562112, India.

Abstract: The effects of precipitation pH values on the electrochemical properties of β -nickel hydroxide materials synthesized by co-precipitation method have been investigated. The β -phase of the synthesized nickel hydroxide materials have been confirmed by x-ray diffraction studies. The structural characteristics such as crystallite size, degree of crystallinity, and capacitance of the electrode of the synthesized β -Ni(OH)₂ are strongly dependent on the pH values of the co-precipitation reaction. The cyclic voltammetry (CV) studies clearly indicate the success of the pH factor by increasing the reversibility of the electrode reaction with a raise in the proton diffusion co-efficient within the nickel electrode. The R_{ct} and capacitance of the electrodes have been fit to the equivalent circuit in the EIS spectrum. An attempt has also been made to examine the relationship between structural characteristics and the electrochemical activity of Ni(OH)₂. Finally, at pH 10, the β -Ni(OH)₂ electrode sample exhibits a lesser R_{ct} value compared to its capacitance.

Keywords: β -Ni(OH)₂; pH; cyclic voltammetry; diffusion co-efficient; electrochemical impedance spectroscopy; charge-transfer resistance;

I. Introduction

Over the past five decades, electrochemical studies of nickel oxide materials have been carried out extensively because of their excellent conducting properties that are useful for secondary batteries. Among them, Ni-MH and Ni-Cd materials are recognized as ideal candidates for battery applications because of their specific energy, sensible cycle ability and high specific power. In addition, the reaction temperature, pH and methods of preparation also play a vital role in modifying the structure and crystallinity of Ni(OH)₂. The changes in the structure, morphology and composition of Ni(OH)₂ leads to the formation of polymorphic crystal structures, generally represented by the unit areas α and β [1]. Every structure has brucite-like layers that are ordered well within the β -phase and randomly stacked within the α -phase. Each structure has brucite-like layers that are requested well inside of the β -phase and arbitrarily stacked inside of the α -phase. Further, α -phase is significantly larger than the β -phase because of the oversized water molecules and anionic species that penetrates into the lattice spacing [2]. Conductor supported α -phase hydroxides unit area possess both lower charge and higher discharge voltages. Surprisingly, the basic media (e.g. KOH) used in batteries revert the α -phase to the β -phase at frequent time intervals. The little auxiliary and electrochemical qualities of β -Ni(OH)₂ materials combined by the co-precipitation technique zone unit intently connected with the amalgamation system parameters, similar preparation temperature, pH of response blend, drying temperature, doping parts and expansion amount of dopant and so on [3]. Among these synthetic parameters, the precipitation pH is a key factor that affects the chemical structure of the crystal, and is subsequently expected to affect the electrochemical characteristics of nickel hydroxide. Therefore, an attempt is made through this paper to study the influence of chemical precipitation reaction pH values on the structure of β -nickel hydroxide materials which has been sparsely investigated in the past. Fig. 1 shows schematic representation of changing the different phases of Ni(OH)₂ with interlayer distance including oxidation state of Nickel. In order to characterize the structure and electrochemical properties of β -Ni(OH)₂ samples, x-ray diffraction (XRD), cyclic voltammetry (CV) and electrochemical impedance spectroscopy (EIS) techniques have been used.

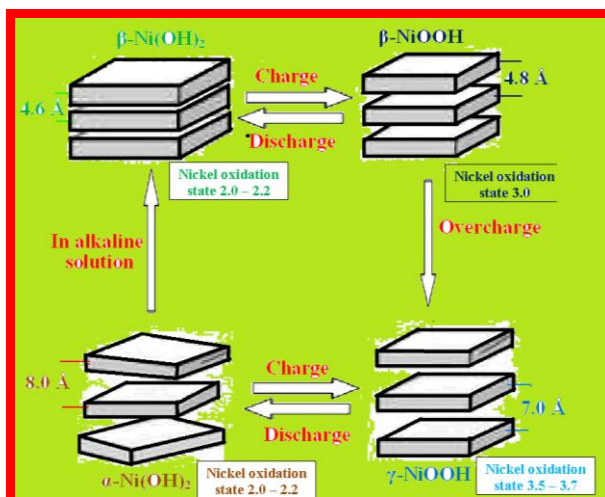


Fig. 1 Different phases of $\text{Ni}(\text{OH})_2$ with interlayer distance including oxidation state of Nickel.

II. Experimental

2.1 Materials

Using the co-precipitation methodology, nickel hydroxides were obtained by dropping 4M NaOH solution into one hundred cubic centimeters of 1M NiSO_4 solution. The samples were prepared at different pH (8, 9, 10 and 11) and the reaction temperature was kept constant at 50 °C. The precipitate was kept for ageing within the mother solution for fifteen hours at 50 °C. Further, by using distilled water, the precipitate was washed until the washed water reached a neutral pH and then the precipitate was dried for 15 hours at 90 °C. A fine powder was obtained by grinding the precipitate and these samples were labeled as given in Table. 1.

Table 1 Name of β - $\text{Ni}(\text{OH})_2$ samples under different pH.

Name of the samples	pH
A	8
B	9
C	10
D	11

80% of the $\text{Ni}(\text{OH})_2$ active material was mixed with 15% of carbon powder to obtain a good quality electrically conducting material. In order to extend the mechanical strength, 5 wt. % of polytetrafluoroethylene (PTFE) was added and ensured that the mixture was in the form of a paste when placed on a nickel mesh (1 cm \times a pair of cm). The conductor material was coated by the paste and dried at 80 °C for 1 h. later; the pasted electrodes were compressed at 20 MPa for 3 minutes to assure smart tangency between the nickel mesh and the active material.

2.2 Characterization

A Philips X'pert-PRO X-ray diffractometer with black lead monochromatized $\text{Cu K}\alpha$ ($\lambda = 1.5418 \text{ \AA}$) radiation was used to obtain the XRD patterns at a scan rate of a 10^0 min^{-1} and 2θ steps of 0.05^0 . For cyclic voltammetry tests, the measurement was performed on a CHI604E potentiostat having a tri-electrode system, consisting of nickel hydroxide electrode, platinum wire and Ag/AgCl as working, counter and reference electrodes respectively. The solution with 6M KOH had a scan rate of 10 mV/s, 20 mV/s, 30 mV/s, 40 mV/s and 50 mV/s and the potential was varied between -1.6 V to 0.6 V (vs. Ag/AgCl electrode). EIS studies were carried out at AC amplitude of 5 mV and a frequency range of 1 Hz to 1 MHz.

III. Result and discussion

3.1 Scanning electron microscopy

The surface of $\text{Ni}(\text{OH})_2$ powder was examined by scanning electron microscope (SEM). Fig. 2 shows the irregular particle shapes exhibited by the synthesized $\text{Ni}(\text{OH})_2$ powder in contrast to the industrial $\text{Ni}(\text{OH})_2$, that are spherical in shape. The irregular shapes could be due to grinding, that has resulted in a greater structural disorder. Nickel hydroxide powders with irregular shapes have a higher specific surface area which will offer a high density of active sites and therefore, promote intimate interaction between the active material and the adjacent electrolyte [4,5].

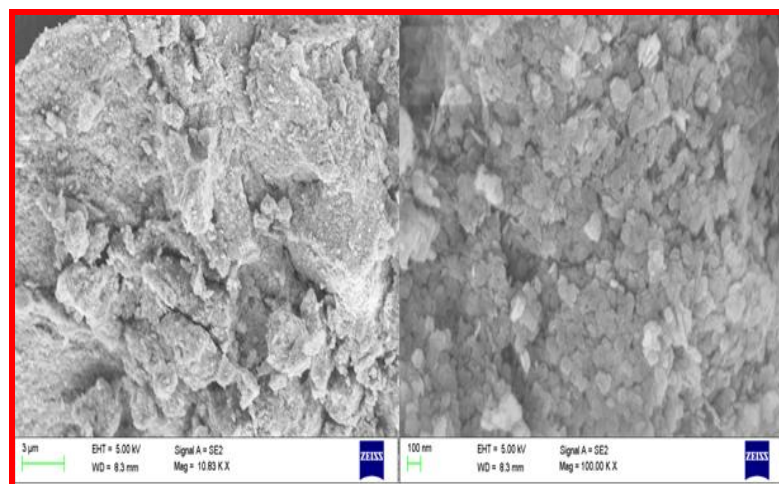


Fig. 2 SEM images of β -Ni(OH)₂ sample.

3.2 X-ray diffraction

The diffraction peaks of the samples at 2θ , 19.30° (0 0 1), 33.10° (1 0 0), 38.70° (1 0 1), 52.10° (1 0 2), 59.10° (1 1 0) and 62.60° (1 1 1) were indexed well and matched with the representatives of nickel hydroxide samples exhibiting characteristics of β -phase with hexagonal brucite structure [3,6-7]. Fig. 3 represents the XRD pattern of the as prepared nickel hydroxide samples. All the x-ray diffraction peaks were indexed to a (space group: P3m1) crystal section of β -Ni(OH)₂, with the lattice constants of $a = 3.130 \text{ \AA}$ and $c = 4.630 \text{ \AA}$, that matches well with the standard literature values (JCPDS card 74-2075). No alternative peaks for the impurities like α -Ni(OH)₂ or alternative phases were determined within the pattern. The broadening of XRD peaks might have resulted from the minute grain sizes or structural small distortions within the crystal [8-9]. Abnormal broadening of the (1 0 l) diffraction lines ($l \neq 0$) within the x-ray pattern cannot be attributed to crystal size alone. Hence, structural defects like stacking faults, growth faults, and/or proton vacancies additionally play a vital role in explaining the effect of broadening [10-11]. Because of the existence of stacking faults within the crystalline lattice of nickel hydroxide powders, the (101) line shows a relationship with the electrochemical activity [12-16]. It was observed that the less ordered nickel hydroxide materials characterized by FWHM of the (101) line of 0.9 (2 θ) exhibits an improved specific capability [12]. The FWHM of the (101) diffraction line of the as-prepared nickel hydroxide sample is 1.966 indicating that the sample possess a high density of structural disorder [4,17]. For the samples C and D synthesized with higher precipitation pH values, the XRD patterns show sharper reflection peaks indicating an increased degree of ordering and crystallinity.

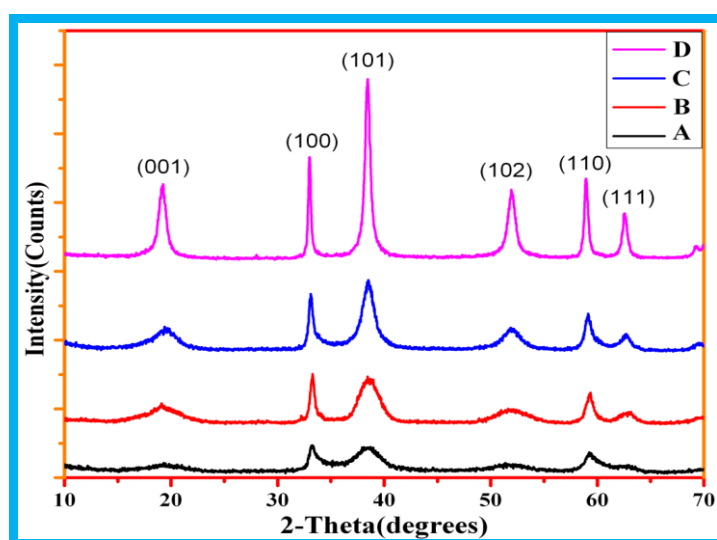


Fig. 3 XRD patterns of samples A, B, C and D.

3.3 Infrared spectra

Fig. 4 presents the infrared spectra of the as-prepared samples A-D. Infrared spectra are helpful in identifying the short-range structure of nickel hydroxide that distinguishes it from the x-ray diffraction patterns resulting from long-range phenomena. As noticeable in IR spectra, all four samples show similar characteristics; the strong, sharp band targeted at 3640 cm^{-1} corresponds to the $\nu(\text{OH})$ vibration, that is typical to IR spectral characteristic of $\beta\text{-Ni}(\text{OH})_2$ [18]. The broad bands around 3300 and 1650 cm^{-1} are of the $\nu(\text{H}_2\text{O})$ stretching vibration and therefore, the $\delta(\text{H}_2\text{O})$ bending vibration of water molecules indicate the presence of a definite quantity of water molecules adsorbable on nickel hydroxide [19]. These water molecules play a very important role in obtaining higher rate-capacity performance of the nickel hydroxide electrodes by providing the necessary passage for hydrogen diffusion on the molecular chain between the layers [20]. The two short bands at 1470 cm^{-1} and 1380 cm^{-1} in each IR spectra may be assigned to the interference from the vibration of carbonate ions [21] because of the open system used for synthesis and the band at 1125 cm^{-1} corresponds to the vibration of SO_4^{2-} ion [22]. The strong, slightly IR optical phenomenon at 520 cm^{-1} can be assigned to $\nu(\text{Ni-OH})$ vibration, and therefore the weak optical phenomenon at 460 cm^{-1} is that of the $\nu(\text{Ni-O})$ stretching vibration mode [23].

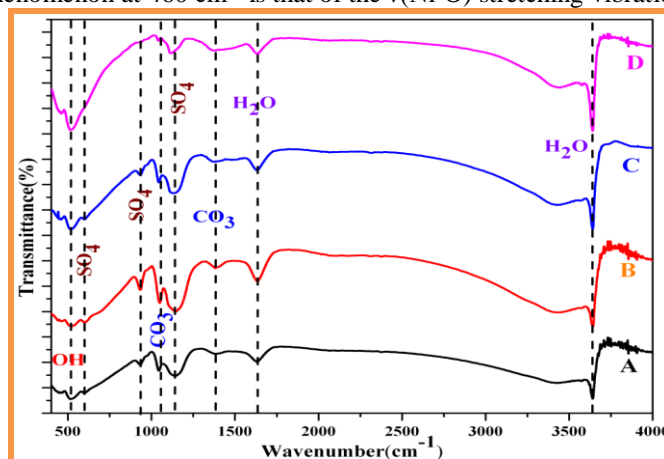


Fig. 4 FT-IR spectra of samples A, B, C and D.

3.4 Cyclic voltammetry

Fig. 5 corresponds to the cyclic voltammograms of $\beta\text{-Ni}(\text{OH})_2$ samples at different pH. The form of the curve indicates that the determined characteristic capacitance is distinct from that of the electrical double layer capacitor, which might turn out to represent a CV curve that may sometimes be close to a perfect rectangle. According to the Randles-Sevcik equation [24], the height current is symbolized by

$$ip = 2.69 \times 10^5 \times n^{3/2} \times A \times D^{1/2} \times C_0 \times v^{1/2} \quad (1)$$

where number of electron transferred in the reaction, extent of the electrode, diffusion co-efficient, scanning rate and initial concentration of the chemical are denoted by n , A , D , v , and C_0 severally. For the $\beta\text{-Ni}(\text{OH})_2$ electrode,

$$C_0 = \rho/M \quad (2)$$

Where the theoretical density of $\beta\text{-Ni}(\text{OH})_2$ and also the molar mass of $\text{Ni}(\text{OH})_2$ are pictured by ρ and M severally. Exploitation the slope of the fitted line in Fig. 5 and Equation (1), the hydrogen diffusion co-efficient for samples A, B, C and D, the hydrogen diffusion coefficients are calculated.

Fig. 6 shows the association between the electrode peak current (ip) and also the square root of the scan rate ($v^{1/2}$) for all β -nickel hydroxide electrodes. The linear relationship between information processing and $v^{1/2}$ confirms that the electrode reaction of $\beta\text{-Ni}(\text{OH})_2$ is controlled by hydrogen diffusion [25]. The hydrogen diffusion co-efficient for sample C is calculated to be $5.415 \times 10^{-6}\text{ cm}^2\text{s}^{-1}$ that is relatively larger than for samples A, B and D (2.022×10^{-6} , 4.287×10^{-6} and $2.780 \times 10^{-6}\text{ cm}^2\text{s}^{-1}$). The upper hydrogen diffusion co-efficient and lower charge transfer resistance in high-density nickel hydroxide is a result of fewer intercalated anions (e.g., SO_4^{2-} , CO_3^{2-}), additional compact structure, high structural disorder density, and high specific capacity. The high density of structural disorder for nickel hydroxide powder is helpful for the acceleration of solid-state hydrogen diffusion within the $\text{Ni}(\text{OH})_2$ lattice and can diminish the concentration polarization of protons throughout charge and discharge, resulting in higher charge-discharge physical behaviour [5]. Moreover, non-spherical nickel hydroxide with a high surface area will offers good interconnectivity network between the nickel hydroxide particles, and optimum degree of contact between the nickel electrode and the solution, which might facilitate the fast movement of electrons and ions within the electrode.

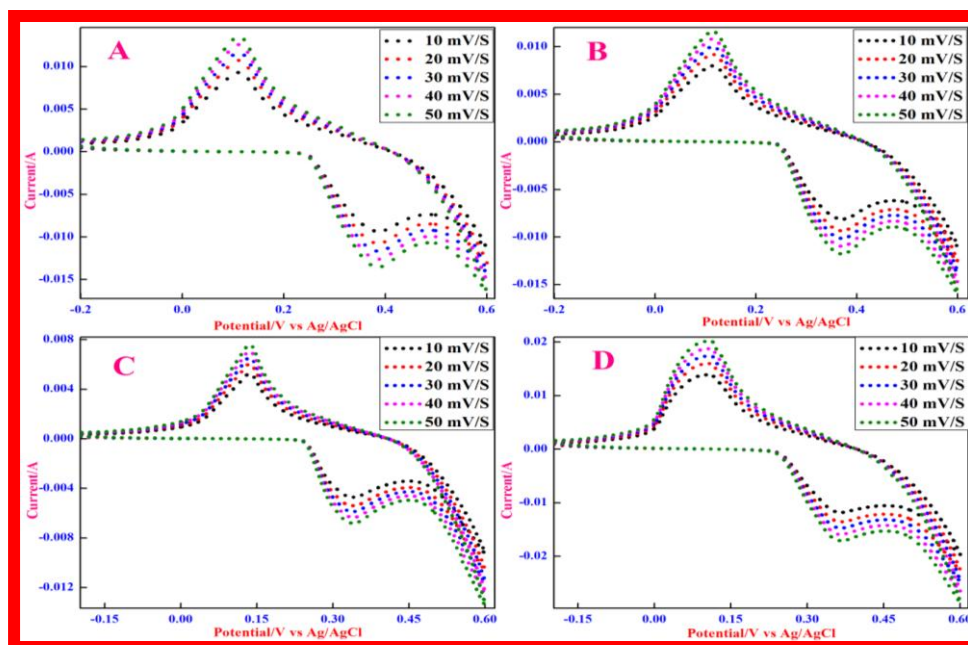


Fig. 5 Cyclic voltammograms of different β -Ni(OH)₂ samples.

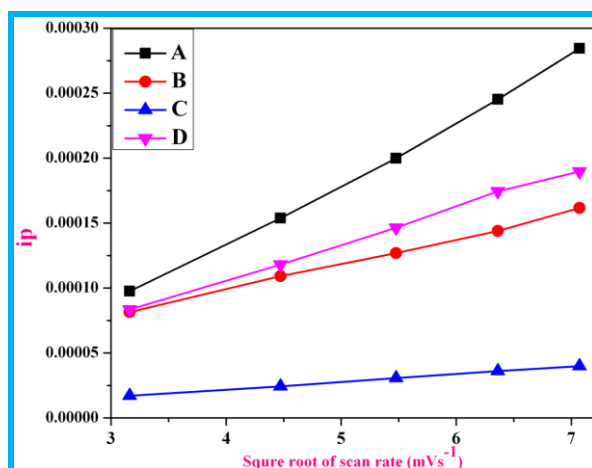


Fig. 6 Relationship between the cathodic peak current (i_p) and the square root of the scan rate for samples A, B, C and D.

3.5 Electrochemical impedance spectroscopy

The impedance spectra of these electrodes show a depressed two-dimensional figure ensuring charge transfer resistance within the high-frequency region, and a slope associated with Warburg resistance within the low-frequency region [25-27], Fig. 7 presents the electrochemical impedance spectra for electrodes A-D at steady state. The resistance of electrode C is far smaller than that of electrode A, B or D, which means that the electrochemical reaction on electrode C precedes a lot simpler than on electrode A, B or D. This can be additionally related to the charge transfer resistance (R_{ct}) and double layer capacitance (C) values obtained from fitting circuits (Fig. 7) for impedance spectra, as given in Table 2.

In Fig. 8, W represents Warburg part that is within the low-frequency region of impedance spectra; Q_1 represents the constant section that is parallel to the charge-transfer resistance (R_{ct}) and also the low frequency capacitance (Q_2), and is additionally parallel to the outflow resistance (R_f) [28]. In general, for a plate-like electrode, the Warburg slope is proportional to $1/CD^{1/2}$ and is about 45° wherever C is the concentration of diffusive species and D is that the hydrogen diffusion co-efficient. This model is satisfactory for a straight forward reaction on plate-like electrodes however; it isn't adequate for a lot of difficult reactions and porous electrodes [29]. The behavior of an electrode with a porous electrode is more complicated. The Warburg slope of a porous electrode is between about 22.5° and 45° , based on characteristics of an electrode with semi-infinite

pores [30]. It is seen from Fig. 7 that the behavior of conductor C is comparable to a plate-like electrode. The charge transfer resistance (R_{ct}) and double layer capacitance (C) values measures the two-dimensional figure at high frequencies as observed in the resistance plot. From these plots, it is clear that the charge transfer resistance is low in sample C compared to samples A, B and D, followed by a rise in the capacitance of the sample C. From these knowledge we will clarify that the electrochemical behavior is a lot of once β -Ni(OH)₂ samples ready in pH scale 10.

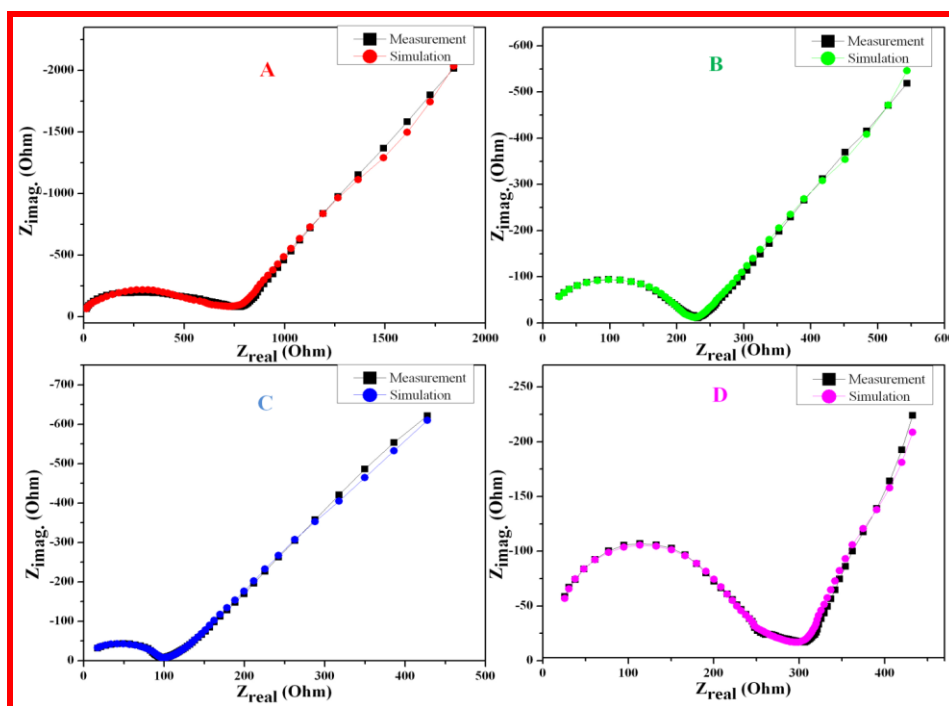


Fig. 7 Electrochemical impedance spectra of samples A, B, C and D.

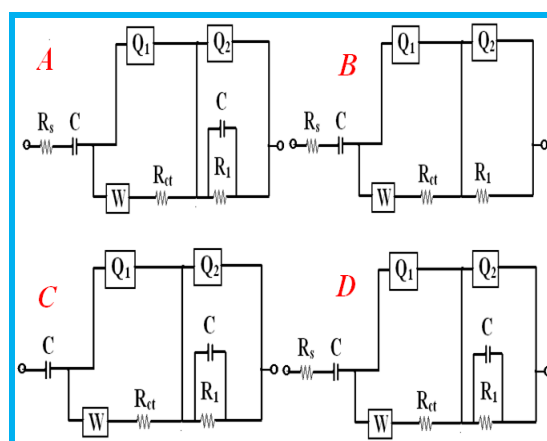


Fig. 8 Equivalent circuits of impedance spectra for samples A, B, C and D.

Table 2 Impedance parameters of different β -Ni(OH)₂ samples by using equivalent circuit.

Name of the Samples	R_{ct}/Ω	C_{dl}/F
A	198.53	0.000358
B	152.4	0.000585
C	22.18	0.01742
D	799.8	1.998×10^{-6}

V. Conclusion

β -nickel hydroxide was prepared by co-precipitation method at different pH values. The structure and property of the synthesized nickel hydroxide were characterized by SEM, XRD. XRD studies processed that the ready nickel hydroxide samples square measure in β -phase. The electrochemical properties of the synthesized β -Ni(OH)₂ materials were analyzed with cyclic voltammetry (CV) and electrochemical impedance spectrometry (EIS). The CV studies clearly indicate that the pH scale issue was pleasing in growing the changeability of the electrode reaction by increasing the hydrogen diffusion co-efficient at intervals the nickel electrode. The R_{ct} and capacitance of the electrodes were recognized by fitting the equivalent circuit for EIS spectrum. R_{ct} of β -Ni(OH)₂ electrode was found to be lower compared to the capacitance wherever pH of Ni(OH)₂ sample was 10.

Acknowledgement

The authors RCR, HPN, SCP and MRA thanks to VGST, Govt. of Karnataka, India, (No: VGST/CISEE/2014-15/282) and (VGST/K-FIST-L1/2014-15/GRD-360) for extended to carry out this research work.

References

- [1] P. Oliva, J. Leonardi, J.F. Laurent, C. Delmas, J.J. Braconnier, M. Figlarz, F. Fievet, A.D. Guibert, J. Power Sour. 8, 1982, 229.
- [2] B. Ash, J. Kheti, K. Sanjay, T. Subbaiah, S. Anand, R.K. Paramguru, Hydrometallurgy 84, 2006, 250-255.
- [3] T.N. Ramesh, P. Vishnu Kamath, Electrochimica Acta 53, 2008, 8324-8331
- [4] Q.S. Song, C.H. Chiu, S.L.I. Chan, Electrochim Acta 51, 2006, 6548-55.
- [5] Q.S. Song, C.H. Chiu, S.L.I. Chan, J. Solid State Electrochem. 12 (2008) 133-41.
- [6] P.V. Kamath, M. Dixit, L. Indira, A.K. Shukla, V.G. Kumar, N. Munichandraiah, J. Electrochem. Soc., 141, 1994, 2956.
- [7] L. Indira, M. Dixit, P.V. Kamath, J. Power Sour. 52, 1994, 93.
- [8] S. Cabanas-Polo, K.S. Suslick, A.J. Sanchez-Herencia, Ultrason. Sonochem. 18, 2011, 901.
- [9] S. Nathira Begum, V.S. Muralidharan, C. Ahmed Basha, Int. J. Hydrogen Energy 34, 2009, 1548.
- [10] Z. Chang, Y. Zhao, Y. Ding, J. Power Sources 77, 1999, 69.
- [11] T.N. Ramesh, P.V. Kamath, Bull. Mater. Sci. 31, 2008, 169.
- [12] U. Kohler, C. Antonius, P. Bauerlein, J. Power Sources 127, 2004, 45.
- [13] C. Tessier, P.H. Haumesser, P. Bernard, C. Delmas, J. Electrochem. Soc. 146 (6), 1999, 2059.
- [14] T.N. Ramesh, P. Vishnu Kamath, Mater. Res. Bull. 43, 2008, 2827-32.
- [15] J. Balej, Int. J. Hydrogen Energy 10, 1985, 365.
- [16] W.G. Zhang, W.Q. Jiang, L.M. Yu, Z.Z. Fu, W. Xia, M.L. Yang, Int. J. Hydrogen Energy 34 (1), 2009, 473.
- [17] H. Chen, J.M. Wang, T. Pan, H.M. Xiao, J.Q. Zhang, C.N. Cao, Int. J. Hydrogen Energy 28, 2003, 119.
- [18] L. Demourgues-Guerlou, C. Delmas, J. Power Sources 45, 1993, 281-89.
- [19] Y.L. Zhao, J.M. Wang, H. Chen, T. Pan, J.Q. Zhang, C.N. Cao, Int. J. Hydrogen Energy 29, 2004, 889-96.
- [20] W.K.Hu, X.P. Gao, D. Nore'us, T. Burchardt, N.K. Nakstad, J. Power Sources 160, 2006, 704-10.
- [21] P. Jeevanandam, Y. Kolytyn, A. Gedanken. Nano Lett. 1, 2001, 263-326.
- [22] N.V. Kosova, E.T. Devyatkina, V.V. Kaichev, J. Power Sources 174, 2007, 735-40.
- [23] F. Portemer, A.D. Vidal, M. Figlarz, J. Electrochem. Soc. 139, 1992, 671-78.
- [24] A.H. Zimmerman, P.K. Effa, J. Electrochem. Soc. 131, 1984, 709-13.
- [25] V. Mancier, A. Me'trot, P. Willmann, Electrochim Acta 41, 1996, 1259-65.
- [26] B. Liu, H.T. Yuan, Y.S. Zhang, Int. J. Hydrogen Energy 29, 2004, 453-58.
- [27] Y.W. Li, J.H. Yao, C.J. Liu, W.M. Zhao, W.X. Deng, S.K. Zhong, Int. J. Hydrogen Energy 35, 2010, 2539-45.
- [28] M.R. Sarpoushi, M. Nasibi, M.A. Golozar, M.R. Shishesaz, M.R. Borhani, S. Noroozi, Mat. Science in Semiconductor Processing 26, 2014, 374-378.
- [29] X.Y. Wang, J. Yan, H.T. Yuan, Y.S. Zhang, D.Y. Song, Int. J. Hydrogen Energy 24, 1999, 973-80.
- [30] S.A. Karunathilaka, N.A. Hampson. J. Appl. Electrochem. 11, 1981, 365.